Human Molecular Genetics, 2015, Vol. 24, No. 4 **926–938**
doi:10.1093/hmg/ddu505
Advance Access published on October 6, 2014

Activating PIK3CA alleles and lymphangiogenic phenotype of lymphatic endothelial cells isolated from lymphatic malformations

Alexander J. Osborn[1,2], Peter Dickie[1], Derek E. Neilson[3], Kathryn Glaser[1], Kaari A. Lynch[1], Anita Gupta[4] and Belinda Hsi Dickie[1,*]

[1]Hemangioma and Vascular Malformation Center, Division of Pediatric General and Thoracic Surgery, Cincinnati Children's Hospital and Medical Center, MLC 2023, 3333 Burnet Avenue, Cincinnati, OH 45229-3039, USA, [2]Division of Otolaryngology, Head and Neck Surgery, Cincinnati Children's Hospital and Medical Center, 3333 Burnet Avenue, Cincinnati, OH 45229-3039, USA, [3]Division of Human Genetics, Cincinnati Children's Hospital and Medical Center, MLC 4006, 3333 Burnet Avenue, Cincinnati, OH 45229-3039, USA and [4]Department of Pathology, Cincinnati Children's Hospital and Medical Center, MLC 1035, 3333 Burnet Avenue, Cincinnati, OH 45229-3039, USA

Received June 10, 2014; Revised and Accepted September 29, 2014

Lymphatic malformations (LMs) are developmental anomalies of the lymphatic system associated with the dysmorphogenesis of vascular channels lined by lymphatic endothelial cells (LECs). Seeking to identify intrinsic defects in affected LECs, cells were isolated from malformation tissue or fluid on the basis of CD31 and podoplanin (PDPN) expression. LECs from five unrelated LM lesions were characterized, including cells derived from one patient previously diagnosed with CLOVES. CLOVES-related LECs carried a known, activating mutation in *PIK3CA* (p.H1047L), confirmed by direct sequencing. Activating *PIK3CA* mutations (p.E542K and p.E545A) were identified in lesion-derived cells from the other four patients, also by direct sequencing. The five LM-LEC cultures shared a lymphangiogenic phenotype distinguished by PI3K/AKT activation, enhanced sprouting efficiency, elevated VEGF-C expression and COX2 expression, shorter doubling times and reduced expression of angiopoietin 2 and CXCR4. Nine additional LM-LEC populations and 12 of 15 archived LM tissue samples were shown to bear common *PIK3CA* variants by allele-specific PCR. The activation of a central growth/survival pathway (PI3K/AKT) represents a feasible target for the non-invasive treatment of LMs bearing in mind that background genetics may individualize lesions and influence treatments.

INTRODUCTION

Vascular malformations are a non-tumorous subset of vascular anomalies thought to arise through developmental dysmorphogenesis. Accompanying refinements in the clinical classification of vascular malformations has been the identification of associated gene mutations (for a comprehensive review 1). Fast-flow malformations affect arteries alone, vessels of mixed arterial-venous identity (AVM) and AVMs with lymphatic and/or capillary involvement (2,3). These have been causally linked to autosomally dominant mutations affecting growth-regulating genes such as *RASA1* and *phosphatase and tensin homolog* (*PTEN*), and specification genes such as endoglin (*ENG*) and *ALK1* (1,3). Alternatively, slow-flow lesions affect capillaries, veins and lymphatics individually or in combination. Mutations in *GNAQ* and *TIE2*, the majority of which are somatically acquired, have been linked to port-wine stains (capillary malformations) and venous malformations, respectively (4,5). Inherited mutations in multiple genes (*KRIT1*, *PDCD10* and malcavernin) have been implicated in the capillary anomaly cerebral cavernous malformation (1,3). Mutations in lymphatic-specific genes such as *FOXC2*, *FLT4* and *SOX18* have been associated with inherited forms of lymphedema (1,6), but an etiopathologic basis remains to be established for lymphatic

*To whom correspondence should be addressed at: Pediatric General and Thoracic Surgery, Cincinnati Children's Hospital and Medical Center, MLC 2023, 3333 Burnet Avenue, Cincinnati, OH 45229-3026, USA. Tel: +1 5136363240; Fax: +1 5136367657; Email: belinda.dickie@cchmc.org

malformations (LMs). The appearance of LMs in syndromic overgrowth conditions does, however, implicate growth-regulating genes (see later).

LMs are congenital lesions comprised dilated lymphatic channels or fluid-filled cysts. Lesions occur sporadically anywhere in the body though most occur in the head and neck region. They can be localized, multifocal or diffuse, extending into the chest, abdomen and limbs. They do not regress but grow proportionally with the growth of the child. Clinical descriptions reflect the nominal size of the lymphatic channels, microcystic versus macrocystic (1,7), or its complexity in terms of vascular involvement. For example, they can be limited to lymphatic vessels, have a venous component (veno-lymphatic malformation, VLM), or be associated with a mixed capillary-venous malformations (capillary-venous-lymphatic malformation, CVLM). Though relatively rare, LMs can be associated with significant pain and morbidity if infiltrative. Traditional treatment options are supportive and based on treating the symptoms of the patient. These include compression, sclerotherapy and debulking surgery. Chemotherapeutic treatments (sirolimus, for example) are currently being evaluated in clinical trials as a means to reduce lymphatic bulk and minimize complications such as infections, pain and fluid leakage (8). Identifying the genetic basis of disease will expand avenues of therapeutic intervention, as will clarifying the cellular basis of LMs. Presently, the affected cell type could be lymphatic endothelium, an endothelial precursor, a vascular stromal cell or even an embryonic cell linked to the perturbation of vessel architecture and lymphatic flow (9,10).

Lymphatic anomalies are a feature of related overgrowth syndromes in which known gene mutations are a determining factor. This provides a clue to the molecular and cellular factors underlying the development of LMs. LMs are a common component of CLOVES (congenital lipomatous asymmetric overgrowth of the trunk with lymphatic, capillary, venous, and combined-type vascular malformations, epidermal nevi, and skeletal anomalies) (OMIM612918), Klippel-Trenaunay (KTS; OMIM149000) and Proteus (OMIM176290) syndromes, all of which have been linked to mutations affecting the receptor tyrosine kinase–PI3K–AKT growth pathway (11–14). Alternatively, lymphatic dysplasia, vessel dilation and lymphangiectasia has been associated with two other syndromes, Noonan (OMIM163950) and Parkes Weber (OMIM608355), linked to mutations in the RAS–MEK–ERK growth pathway (15,16).

Our objective was to explore the lymphangiogenic profile of lesion-derived lymphatic endothelial cells (LM-LECs) as a basis of disease. Loosely overlapping LECs line the fenestrated capillaries of the distal lymphatic system. These take up interstitial fluid and immune cells which are propelled through muscularized collecting lymphatic tubules. Unidirectional flow is maintained by the existence of valves in the collecting vessels as fluid is moved through draining lymph nodes and returned to the central circulation (17). The principal drivers of embryonic and post-natal lymphatic growth are VEGF-C and VEGF-D acting through the VEGFR3 receptor whose activation triggers signals via major growth/survival pathways mediated by PI3K/AKT and RAS/ERK (18). Numerous auxiliary gene products regulate lymphatic growth and may contribute to vessel dysmorphogenesis. These include angiopoietins 1 and 2, VEGF-A, basic fibroblast growth factor and hepatocyte growth factor. The elaboration of factors such as CXCL12 (SDF-1), platelet-derived growth factor and insulin-like growth factor 1 may influence lymphangiogenesis indirectly through VEGF induction or pericyte recruitment (17). It is in the context of these factors that we evaluated the lymphangiogenic potential of LECs from five independent patient lesions. Furthermore, this phenotype was related to the presence of somatically acquired activating *PIK3CA* mutations present in each lesion.

RESULTS

Clinical and cellular features of LMs and derived LECs

With the approval of the Institutional Review Board at the Cincinnati Children's Hospital and Medical Center, we obtained de-identified tissue samples from patients who had undergone surgical or sclerotherapy treatment for LMs. Lesions included lymphatic blebs, microcystic samples or large macrocystic lesions accompanying overgrowth conditions (Fig. 1A). Patient 558 was diagnosed with CLOVES, and underwent surgery to debulk a substantial truncal LM with fatty overgrowth. Patient 837 was diagnosed clinically and radiologically with a CVLM with soft tissue overgrowth affecting the left pelvis and leg. Boney overgrowth was associated with the left foot. Fluid aspirate was obtained from a large gluteal cyst. Patient 935 was diagnosed with CVLM affecting the trunk, left pelvis and leg. No boney overgrowth was noted. Thromboses and post-contrast enhancement, indicating a venous component, were seen by MRI. The source of tissue was a debulked pelvic LM. Patient 1152 was diagnosed with a mixed (micro- and macrocystic) LM of the lower abdomen, buttocks, upper thigh and genital region, for which surgical debulking was performed. Finally, patient 1165 underwent surgery to debulk a microcystic lesion of the tongue, neck and pharynx. Radiographic examination confirmed the diagnosis of LM.

Resected lesions were examined histologically to verify their identity as LMs. In the case of patient 837, cells were isolated from cystic fluid aspirates prior to sclerotherapy, and a histologic examination was not performed. In the four remaining cases, there was extensive infiltration of stromal tissue by dilated lymphatic channels lined with PROX1-positive cells (Fig. 1B, left panel). PROX1 is a definitive marker for LECs (19). Immunostaining for αSMA highlighted the unusual and variable muscularization of lymphatic vessel walls typical of these lesions (Fig. 1B, right panel). Following tissue disaggregation or centrifugation of aspirated cells, cell populations were expanded in endothelium growth medium (EGM-2MV, Lonza) and fractionated by immunomagnetic separation on the basis of CD31 expression. CD31-positive endothelial cells were predominantly PROX1-positive, revealing cell populations consisting mostly of LECs. A second selection was performed on the basis of PDPN expression (20), producing homogeneous populations of PROX1- and PDPN-positive LECs (Supplementary Material, Fig. S1). The cell morphology displayed by the LM-LEC populations was similar to that of the normal dermal LECs (dLyNeo cells) used as control cell populations for our comparative analyses (not shown).

Prior to genetic investigations, we sought evidence of growth or functional anomalies in comparisons with normal dermal LECs. Doubling times of the isolated LM-LECs varied widely

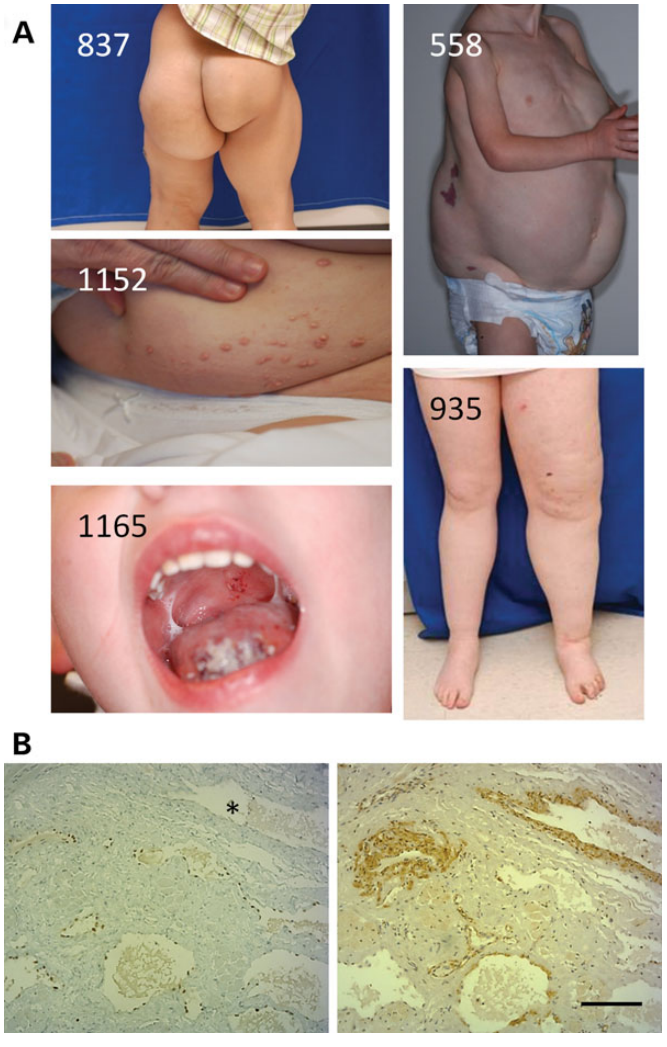

Figure 1 Source of LMs and representative immunohistochemistry. The five patients included in the study, revealing the LMs that were the source of lesion tissue, are shown in (**A**). Serial sections from a malformation removed from the tongue of a patient (1165) are shown in (**B**). (B, left panel) Staining for PROX1 highlights the dark nuclei of LECs lining the lumen of dilated vessels. The asterisk marks a vessel negative for PROX1 staining. In the right panel, a serial section is stained for αSMA, demonstrating continuous, even staining for smooth muscle actin characteristic of veins (upper right, corresponding to vessel with asterisk). This contrasts with the variable, discontinuous staining of cells associated with lymphatic vessels. The scale bar is 200 μm. Counterstained with hematoxylin.

(Table 1), but accelerated growth was evident in four of the five LM-LEC populations. Enhanced lymphangiogenic capacity was exhibited in spheroid sprouting assays conducted in the presence or absence of vascular endothelial growth-factor C (Fig. 2A and B). Spheroids of dLyNeo cells embedded in collagen gels failed to sprout in the absence of exogenous growth factors, whereas sprouting was visible from spheroids of each LM-LEC population when cultured in growth-factor-free medium (Red2MV). Supplementation of Red2MV with VEGF-C promoted sprouting from dLyNeo spheroids and further enhanced the sprouting from spheroids of LM-LECs. Enhanced proliferation and sprouting, and the reduced dependence on exogenous growth factors attested to the heightened lymphangiogenic potential of LECs from patient malformations. These acquired attributes of LM-LECs, passaged free of stromal cell influence, were deemed likely to reflect an intrinsic genetic change.

Gene sequencing of lesion-derived LECs

A genetic basis for the heightened lymphangiogenic sprouting of LM-LECs was explored. Patient 558, having been diagnosed with CLOVES, was expected to bear a mutation in *PIK3CA* based on the recent association of activated *PIK3CA* alleles with CLOVES (11). We confirmed the presence of an activating *PIK3CA* allele, c.3140A>T (p.H1047L), in our CLOVES (558) cell population by direct PCR sequencing (Fig. 3A, based on RefSeq. NM_006218.2). Mutant and wild-type sequences overlap at the position of the exchanged base indicative of allele heterozygosity. The mutation was not present in the non-endothelial cell population derived from the same patient (Fig. 3A) indicative of its mosaic presence.

Given the similar phenotype shared by the five LM-LEC populations, we screened all samples for the presence of activating *PIK3CA* alleles. LM-LEC genomic *PIK3CA* sequences spanning known mutation hotspots (corresponding to codons E542, E545 and H1047) were amplified as previously described (11), and sequenced. Common *PIK3CA* variants were discovered in all cell populations. Patient 1152 LECs carried a *PIK3CA* mutation at c.1634A>C, yielding a known oncogenic p.E545A substitution (21) (Fig. 3A). LM-LECs from patient 837 carried another *PIK3CA* allele (c.1624G>A, p.E542K). The analysis of LECs from patients 1165 and 935 also revealed c.1624G>A/ p.E542K mutations. For these latter two samples, the mutant allele was not detected in their CD31-negative co-isolated cell counterparts (not shown), indicative of tissue mosaicism.

For the rapid identification of *PIK3CA* alleles in lesion samples, we developed an allele-specific PCR assay based on the amplification-refractory mutation system (ARMS-PCR). Primer pairs were designed to detect the four oncogenic alleles already identified in LMs, and a fifth common activating allele with an H1047R substitution. The presence of the *PIK3CA* (E545A) allele in three random 1152 LM tissue samples was demonstrated by this technique (Fig. 3B). A weak positive signal relative to the CD31-selected LM-LECs is consistent with allele mosaicism. Separately, the p.E542K allele was detected in samples of 837 cells, 935 tissue and 1165 tissue (Fig. 3B, right panel). Sequential dilution of *PIK3CA* p.E542K sequences (present in LM-LEC 837 DNA) with genomic DNA bearing wild-type sequence, gave an indication of the sensitivity of ARMS-PCR in these screens. Levels of allele mosaicism in the 1–5% range were reliably detected. Allele mosaicism was indicated for 935 and 1165 lesion samples as evinced in comparisons of LM-LEC cultures with lesion tissue. Interestingly, there was an apparent difference in E542K *PIK3CA* allele abundance among 837, 935 and 1165 LM-LEC cultures. To explore this possibility further, relevant *PIK3CA* sequences from 1165 and 935 genomic DNA were PCR amplified, cloned and sequenced. Nine of 25 (36%) 1165 clones, and 8 of 20 (40%) 935 clones, bore the p.E542K allele. Not only did this result suggest a more equal abundance of the *PIK3CA* allele in these two populations, it suggested its heterozygous presence in most cells of the respective cultures (approaching 80% of the cells). While ARMS-PCR is

Table 1 Source and characteristics of LEC populations

Identifier	1152	1165	558	935	837
Race/sex/age[a]	W/F/16	W/M/2	W/F/3	W/F/24	B/M/2
Diagnosis	LM	LM	CLOVES	CVLM	CVLM with overgrowth
LM site	Groin	Tongue	Thoraco-abdominal	Labia	Buttock
Pathology	Irregular vascular channels with lymph material within and various amounts of smooth muscle lining	Irregular vascular channels with lymph material within, lacking smooth muscle	Muscularized lymphatic vessels	Vascular channels with blood or lymph and variable amounts of smooth muscle lining	(No histo)
LEC source	Tissue	Tissue	Tissue	Tissue	Aspirate
dT(+/−GF)[b]	19/40	76/170	24/35	31/80	21/40
PIK3CA allele	E545A	E542K	H1047L	E542K	E542K

Clinical and histopathologic descriptions of the lesions are indicated, as is the source (surgically removed tissue or aspirated fluid) of the LECs.
[a]White/Caucasian (W), Black/African Descent (B), Female (F) and Male (M); age in years.
[b]Doubling times (dT, in h) are reported in EGM-2MV/Red2MV (EGM-2MV with 1% serum and no growth factors). The doubling time for dLyNeo cells was 48 h in EGM-2MV.

a sensitive assay for specific alleles, quantitative comparisons of cells from different genetic backgrounds is unreliable.

Activation of growth pathways in LM-LECs

PIK3CA somatic mutations have been correlated with the hyperactivation of AKT and enhanced cellular growth in the context of CLOVES and cancer (11,21). We investigated the activation of the PI3K/AKT signaling pathway in LM-LECs by measuring levels of constitutive phospho-S473-AKT, versus total AKT, in cell lysates by western blot analysis (Fig. 4A). As expected, based on the presence of activating *PIK3CA* mutations in all of our lesions, the five cell cultures displayed significantly elevated AKT activation (Fig. 4B). The expression of PTEN, a major negative regulator of PI3K activity (22), was assessed for a possible role in PI3K hyperactivation in LM-LECs. We found no evidence for an abnormal down-regulation of PTEN expression at the gene or protein level (Fig. 4A and C).

The steady-state status of ERK activation was explored as a possible contributor to growth enhancement. Vascular endothelial growth-factors signal through MEK/ERK, as well as PI3K (18). Moreover, given the crosstalk between the PI3K/AKT and MEK/ERK pathways, MEK/ERK signaling could have a regulating role in PI3K activity in endothelial cells (23). Cell levels of phosphorylated ERK1/2, indicative of MEK/ERK activation, are shown in Figure 4A and D. Cells from 1165 to 935 displayed elevated ERK activation. However, this was not a common feature of LM-LECs as the other three LM-LEC populations displayed reduced levels of constitutive ERK phosphorylation.

Lymphangiogenic gene expression profiles of isolated LM-LECs

LM-LEC populations were characterized with respect to the expression of lymphangiogenic genes to identify (i) secondary factors contributing to dysregulated growth and (ii) potential biomarkers distinguishing LM-LECs on the basis of their individual mutations. VEGF-C and angiopoietin 2 (ANG2) are lymphangiogenic drivers that signal through PI3K/AKT and MEK/ERK pathways (24,25). In turn, PI3K activation is known to regulate the expression of both these factors (25,26). Transcriptional analyses by qRT-PCR revealed in LM-LECs an elevated level of *VEGFC* expression compared with control LECs. This correlated with generally higher levels of secreted VEGF-C, as detected by ELISA-based measurements of conditioned medium (Fig. 5A and B). If endogenous VEGF-C expression contributed to the observed enhancements in lymphangiogenic activity it would appear to be factor-driven, rather than receptor-driven, as the levels of *VEGFR3/FLT4* transcription were unaltered in LM-LECs (Fig. 5C). Also striking in these cultures was the reduced level of *ANG2* transcription, which correlated with low levels of cell-associated and secreted ANG2 protein (Fig. 5D and E).

Elevated VEGF-C expression contrasted with normal transcriptional levels of VEGF-A and VEGF-D (Fig. 6A and B). VEGF-A and -D can also promote lymphangiogenesis (18,27). Next, we explored the possible involvement of the ligand–receptor pair of CXCL12 (SDF-1) and CXCR4. CXCL12/CXCR4 mediates tube formation and migration of LECs, activating ERK and AKT pathways in the process (28). The modulation of CXCR4 expression in endothelial cells may affect the autocrine–paracrine roles of CXCL12 during vessel maturation (29). CXCR4 transcription was much reduced in all LM-LEC populations, while the expression of its ligand CXCL12 was variable (Fig. 6C and D). Finally, we examined *COX2* expression levels. COX2 converts arachadonic acid to prostaglandin H2, an intermediate in the biosynthesis of prostaglandins that possess angiogenic activity. COX2 has been shown to be associated with enhanced lymphangiogenesis in various tumors (30). In general, mRNA and protein levels of *COX2* were elevated in LM-LEC cultures (Fig. 6E and F). In summary, a mixed lymphangiogenic profile of sustained VEGF-C production, low ANG2 expression, low CXCR4 transcription and elevated COX2 expression was common to the five lesion-derived populations of LECs.

Susceptibility of LEC cultures to cell signaling inhibition

We evaluated the roles of PI3K/AKT/mTOR activation and VEGFR3 activation in the enhanced growth of LM-LECS by measuring the effects of selective inhibitors in cell proliferation

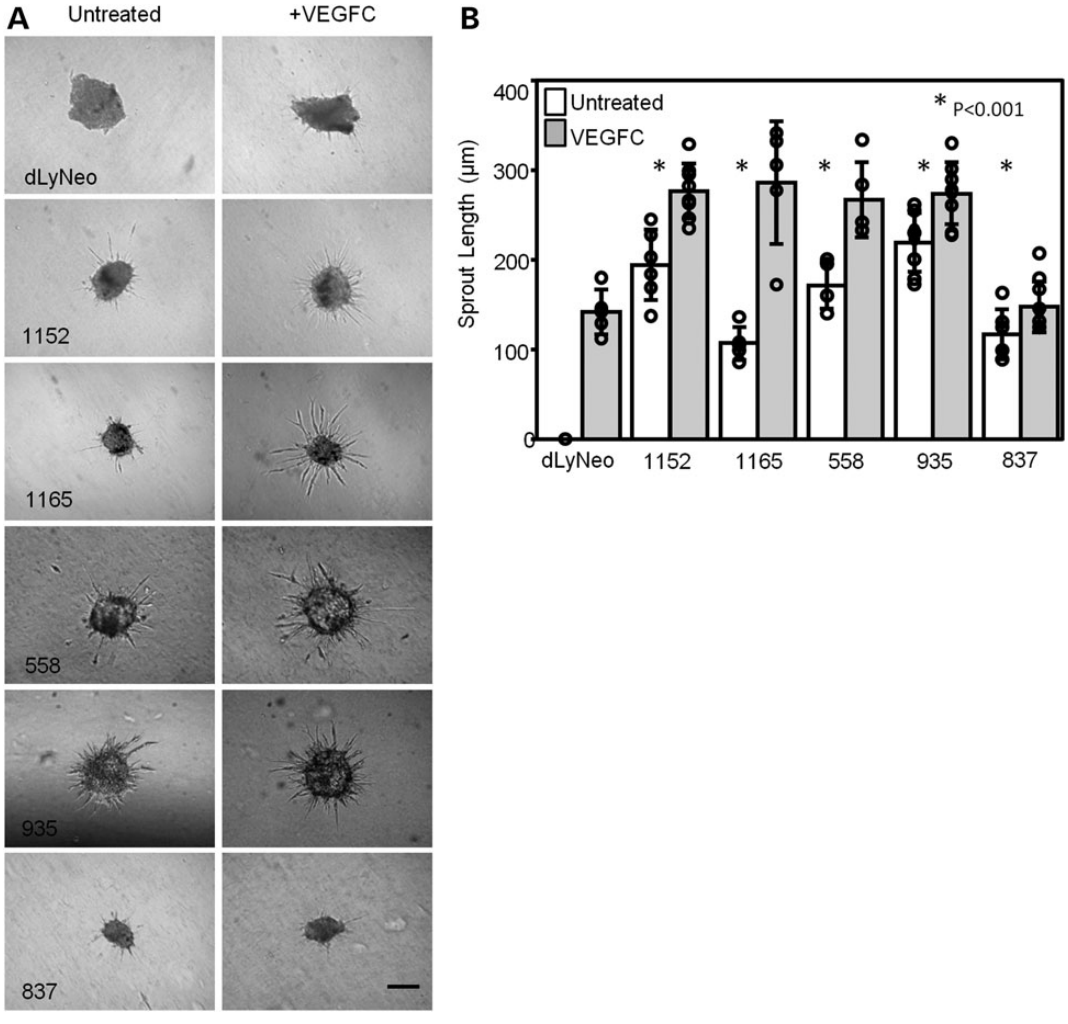

Figure 2 Sprouting lymphangiogenesis of LM-LECs. (**A**) Endothelial cell spheroids formed from 1000 cells were embedded in collagen and overlaid with reduced EGM-2MV (Red2MV) medium alone (untreated) or Red2MV with VEGF-C (100 ng/ml). Sprout lengths were measured after 24 h of culture. Representative spheroids are shown. Scale bar represents 200 μm. (**B**) Average sprout lengths from individual spheroids are plotted and compared ($n = 7$ spheroids).

assays. A potent inhibitor of the PI3K p110α catalytic subunit (GDC-0941) (31) effectively inhibited the proliferation of LM-LECs but with no specificity relative to control LECs (Fig. 7A). In contrast, four of five LM-LEC cultures were more sensitive to the mTOR inhibitor Rapamycin (Sirolimus), a drug with clinical efficacy in the treatment of LMs (8). Downstream of PI3K/AKT, mTOR mediates multiple cell growth signals (23). Cultures of the slower growing 1165 LM-LECs appeared to be less sensitive to this drug than the other LM-LECs (Fig. 7B), though they remained marginally more sensitive than control LECs. Finally, a potent and specific inhibitor of the VEGF-C receptor (VEGFR3), SAR131675 (32) was tested, in part to evaluate the growth contributions of endogenously expressed VEGF-C. The growth of LECs bearing *PIK3CA* mutations was not inhibited by drug concentrations (10^{-8}–10^{-6} M) that effectively inhibited the growth-factor-driven proliferation of normal LECs (Fig. 7C). Measurements of 1165 LM-LEC sensitivity to SAR131675 were unobtainable because of their slow growth in the reduced medium used in these experiments. The relative resistance of LM-LECs to the VEGFR3 inhibitor is an indication that receptor activation is not a significant contributor to enhanced growth in LM-LEC and that endogenously expressed VEGF-C is not likely a major driver of growth in LM-LEC cultures.

Scope of PIK3CA mutations in LMs

To explore the broader significance of *PIK3CA* mutations in LMs, we screened nine more recently derived LM endothelial cell cultures not otherwise characterized in this study, along with samples of LM, VLM and CVLM tissue deposited in our Vascular Anomalies Tissue Repository. Genomic DNA was analyzed by direct sequencing of hotspot regions within the helical domain (E542, E545) and kinase domain (H1047) of PIK3CA (cell cultures only) or by implementing ARMS-PCR to detect mutations related to E542K, E545A, E545K, H1047 R and H1047L alleles (archived tissue). Results for all screened cells and tissues (with the five subjects central to this report) are presented in Table 2. Subjects were grouped by clinical presentation as (i) LM in the head and neck region, (ii) LM on the trunk

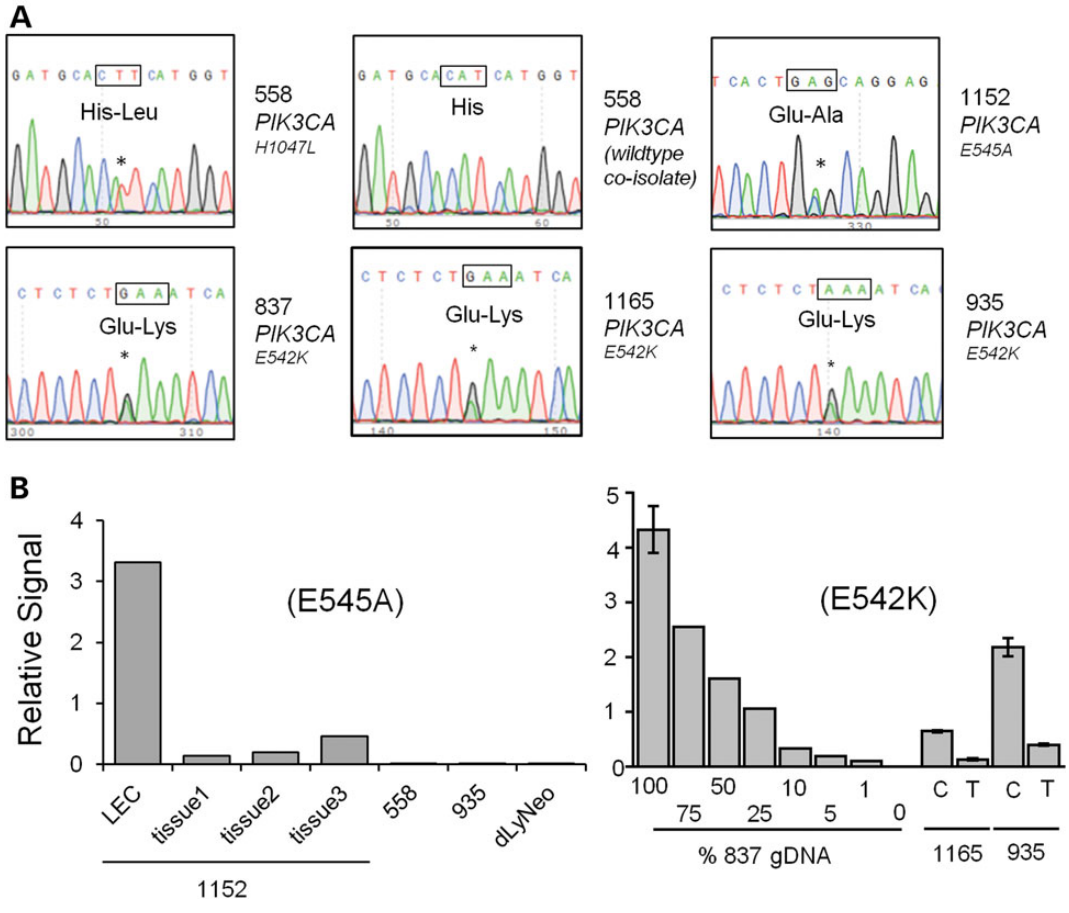

Figure 3 Sequencing of mutant loci associated with LMs. (**A**) The *PIK3CA* alleles of 558, 1152, 1165, 935 and 837 LM-LECs are demonstrated in original sequencing profiles. A wild-type *PIK3CA* sequence is included as it appeared in 558 non-endothelial co-isolated cells. Allele heterozygosity is evident from the double peaks indicated by the asterisk. The resultant mutations are indicated as amino acid substitutions (His to Leu in 558, for example). Computer-generated sequences are included and the affected codons are boxed. (**B**) Allele-specific real-time quantitative PCR for E545A and E542K *PIK3CA* alleles was performed on genomic DNA (gDNA) isolated from the indicated samples. In the left panel, 1152 LECs and 3 random tissue samples are positive for the E545A allele while gDNA from 558, 935 and dLyNEO cell lines is negative. In the right panel, qPCR was performed on gDNA from 837 cells diluted to the indicated proportion with wild-type DNA. The same allele (E542K) was detected in gDNA samples of 935 and 1165 cells (**C**) and tissue (T).

or extremity, (iii) CVLM with no overgrowth and (iv) CVLM with overgrowth. In each case, tissue or cells were derived from debulked or aspirated LMs. All nine recently derived LM-LEC populations bore one of the five common *PIK3CA* alleles. Thus, 14 of 14 derived LEC populations, representing each clinical entity, possessed a common activating *PIK3CA* allele. Among archived samples, 7 of 8 LM and 5 of 7 CVLM samples were positive for an activating *PIK3CA* allele. Only three archived VLM samples were tested and each was negative for the screened mutant alleles.

DISCUSSION

LECs derived from five independent LM (LM-LECs) displayed growth enhancement *in vitro* coincident with an elevation in PI3K/AKT activation. All five LEC populations, and nine more recently derived LM-LEC populations, were discovered to contain genomic mutations in *PIK3CA*, the catalytic p110α subunit of PI3K. The *PIK3CA* mutations identified are allelic hotspots and correlate with PI3K activation (21). In addition, activated *PIK3CA* alleles were detected in 12 of 15 archived tissue samples. In total, 26 of 29 (89%) samples of LM/CVLM tissue were identified bearing activating *PIK3CA* alleles. Our assays were limited to the identification of common hotspot mutations, but not all reported activating alleles. The presence of less common activating alleles may account for the three negative results we obtained with archived LM/CVLM samples. The presence of these common activating *PIK3CA* alleles in LM samples is similar to allele frequencies associated with *PIK3CA*-mutated cancers (33).

The association of LMs with activated PI3K-AKT linked syndromes (CLOVES, KTS and Proteus) is consistent with our association of activated PI3K activity in LMs removed from overgrowth conditions. LMs would appear to be distinct genotypically, as well as phenotypically, from lymphatic anomalies observed in overgrowth syndromes underpinned by activating RAS-MAPK mutations (Parkes Weber and Noonan). In these latter overgrowth syndromes, lymphatic dysplasia and lymphangiectasia were featured (15,16). The absence of LMs in certain *PIK3CA*-related overgrowth syndromes (34) can be expected if the acquired *PIK3CA* alleles occurred in a cell outside the vascular lineage. For non-syndromic LM, we suspect that the

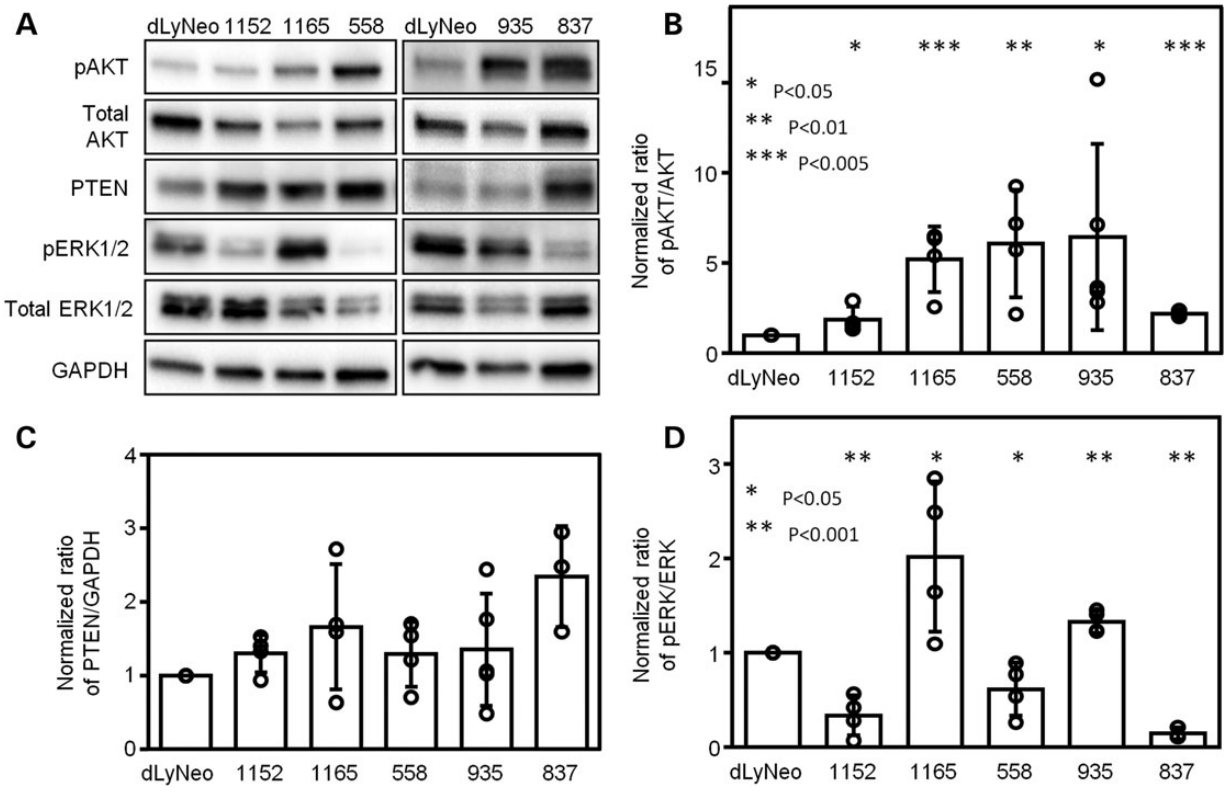

Figure 4 Activation of PI3K/AKT and ERK1/2 signaling pathways in LM-LECs. (**A**) LM-LEC cultures were grown in Red2MV and total protein analyzed by western blot analysis. Blots were stripped and re-probed for each protein product. (**B**–**D**) The results of four independent comparisons were normalized to GAPDH and combined following normalization to values computed for each respective dLyNeo lysate. Standard deviations are indicated. In (B) and (D), all patient-derived samples are significantly different from dLyNeo and *P*-values are displayed above each sample set (paired Student's *t*-test).

acquisition of an activating *PIK3CA* allele occurred late in the differentiation process, within a committed endothelial cell. The endothelial origin of these lesions is in contrast to infantile hemangiomas, in which genetic reprogramming appears to originate in a vascular progenitor cell. These stem cells differentiate into abnormal pericytes which fail to regulate endothelial organization (35). The abnormal lymphangiogenic phenotype, we describe for LM-LECs, is independent of stromal cell/anatomical influence and reflects an inherent pathologic change.

A recent report alludes to a genotype–phenotype association of different *PIK3CA* alleles with clinically distinct segmental overgrowth syndromes [fibroadipose overgrowth (FAO); hemihyperplasia multiple lipomatosis (HHML); macrodactyly, megalencephaly syndrome and CLOVES] (34). Specifically, codon 1047 substitutions (in the catalytic domain of PI3K) were present in 23 of 25 cases of FAO, HHML and macrodactyly as detected in affected bone, adipose tissue, muscle or skin. In contrast, codons 542 and 545 (in the helical domain) were disproportionately substituted in alleles detected in CLOVES patients (6 of 9). As only 15 total subjects manifested vascular malformations, and malformations are a clinical feature of CLOVES, few of the FAO/HHML/macrodactyly group displayed vascular malformations. Hence, codon 1047 mutations were more often associated with overgrowth than vascular malformations. A bias was observed in our data as well. LMs with no associated overgrowth or mixed vascular components predominantly carried helical domain mutations (12/15 LMs, 75% codon 542 and 545 substitutions; Table 2). However, in more complex clinical settings (i.e. CVLM with or without overgrowth), codon 1047 mutations were better represented (55%). These correlations may be related to allele-specific differences in AKT activation and downstream signaling. Allele-specific impact on LEC function, disease progression and susceptibility to treatment requires further investigation.

Our five populations of *PIK3CA*-mutant LECs shared a common lymphangiogenic signature relatable to the overactivation of PI3K/AKT signaling. They exhibited elevated levels of phosphorylated AKT, elevated VEGF-C and COX2 expression, enhanced sprouting activity in the absence of growth factor, reduced ANG2 expression and release, and reduced CXCR4 expression. This profile may explain some of the gross and microscopic characteristics of LMs. The distil lymphatic system is composed of primary lymphatics with a discontinuous basement membrane (absorptive component) and pre-collectors that are both absorptive and propulsive (36). The scattered association of smooth muscle cells on pre-collectors (facilitating propulsion) develops in an AKT- and ANG2-dependent fashion. The PI3K/AKT axis is critical for lymphatic vessel maturation (37) as it perpetuates an activating loop by inducing VEGF-C expression. ANG2, in contrast, is repressed by PI3K activity, involving the phosphorylation-dependent inactivation of FOXO1 and FOXO3a, transcription factors that are essential for ANG2 expression (38). Thus, up-regulated PI3K/AKT signaling in LM-LECs conceivably elevates VEGF-C expression

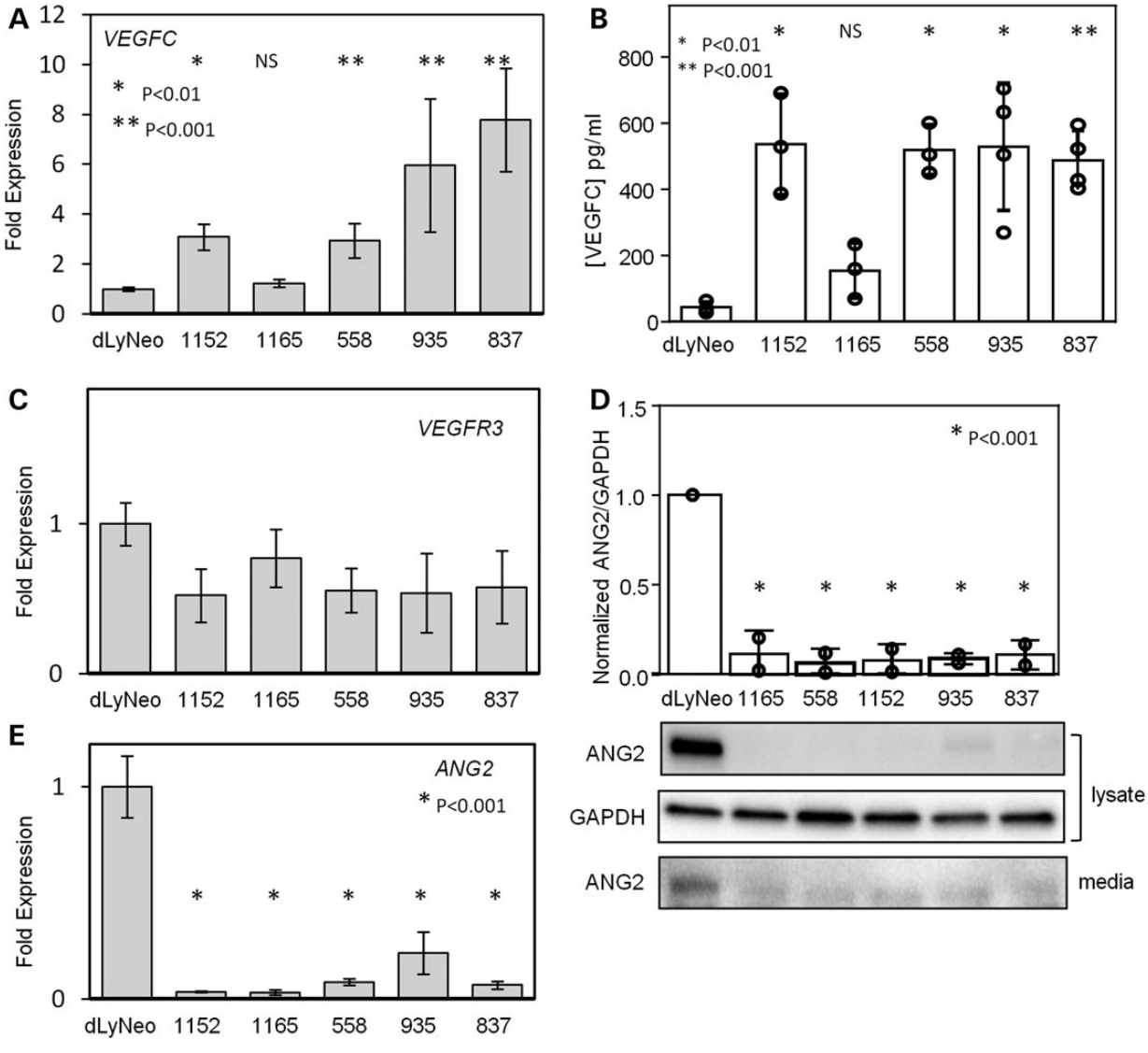

Figure 5 Comparative gene expression in LM-LECs. (**A**) qPCR of LM-LEC cDNA compares levels of *VEGFC* gene expression. Cumulative results of four experimental sets are included. Bars represent standard error of the mean. (**B**) Cell-free VEGFC (measured by ELISA) is compared and bars represent standard deviation. *P*-values are indicated. (**C**) qPCR of LM-LEC cDNA for *VEGFR/FLT4* expression as measured in (A). (**D**) Comparative levels of secreted and cell-associated angiopoetin-2 (ANG2) protein by western blot and (**E**) mRNA expression by qPCR are shown. At least three experiments, consisting of duplicate measurements, are shown and all patient-derived cells are significantly different than dLyNeo and *P*-values are shown. Bars represent standard deviation (*D*) or standard error of the mean (*E*). Student's *t*-test applied in (A) and (B). NS, not significant.

and decreases ANG2 expression, advancing the characteristics of stable, more muscularized vessels. The down-regulation of CXCR4 may be relevant to this process, as shown in maturing blood vessels (29). Vessel dilation and expansion within LMs may be promoted by the overactivation of COX2. PI3K/AKT enhances COX2 expression, by activating the NF-κB transcriptional program (39, 40). In turn, COX-2 promotes lymphangiogenesis via its products, inflammatory prostanoids, which can also induce lymphatic vessel dilation (30).

The potential of LM-LECs to exert a positive paracrine effect on lymphatic vessel growth and activation limits our interpretation of the pathologic impact of *PIK3CA* mutations. It is equally plausible that abnormal vessels are lined exclusively by mutated LECs, or that cells in affected vessels walls are themselves mosaic with respect to *PIK3CA*. In the latter scenario, wild-type LECs could be abnormally activated by factors elaborated by mutant cells. Since abnormal vessels can lie in proximity to normal vessels, our LEC populations were likely mosaic by either scenario in the early stages of isolation. Allele representation in isolated LECs will be influenced further by any intrinsic growth advantage conferred by an activated PIK3CA allele. Hence, allele representation in our cultures may not accurately reflect their representation *in vivo*. The etiopathologic effect of activated *PIK3CA* alleles may be paracrine, intrinsic or permissive.

The LM-LEC cultures 935 and 1165 were distinguished by increases in constitutive ERK1/2 activation. The effect seems unrelated to the acquired *PIK3CA* mutation as 935, 1165 and 837 populations bear the same E542K allele. Furthermore, these cells differ with respect to AKT activation and growth rates. We suspect that differences in background genetics or

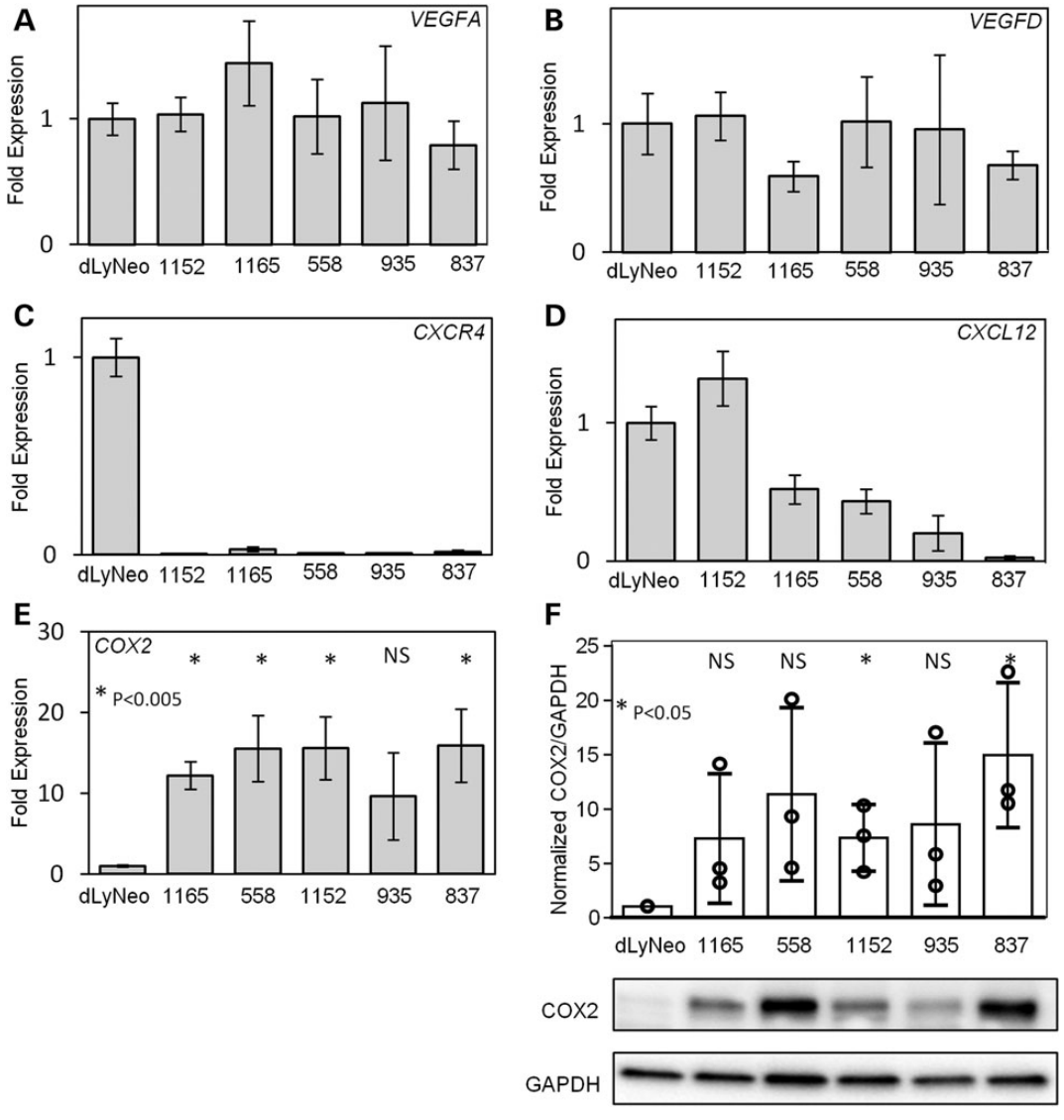

Figure 6 Comparative gene expression profiles of patient LECs. (**A**–**E**) Data collected from four independent experiments, screening for gene expression by qRT-PCR. Data are normalized to levels of expression computed for control dLyNeo LECs. Bars represent standard error of the mean. (**F**) COX2 protein was measured by western blot and levels compared with dLyNeo after normalization to GAPDH. Data from three independent experiments are illustrated and a representative blot is shown. Bars represent standard deviation. Statistical significance was computed by paired Student's *t*-test. NS, not significant.

the presence of additional mutations contribute to phenotypic profiles. Oncogenic activation in the absence of additional permissive mutations can often lead to restrictive cell growth such as through the induction of senescence. Thus, the acquisition of permissive mutations may explain differences in the observed phenotypes of our LM-LEC populations (41). Combined PI3K/AKT and MEK/ERK activation is consistent with lymphangiogenic signaling downstream of VEGFR3 (18). However, LM-LEC cultures were generally insensitive to VEGFR3 inhibition suggesting that receptor activation (inherent or driven by endogenous VEGF-C expression) was not a major contributor to growth in any of the LM-LEC cultures. The contribution of additional mutations to LM-LEC dysfunction remains unresolved.

Variability in the clinical presentation of LMs may be reflected in susceptibility to applied drug treatments. For that reason, LM-LEC cultures will be useful in screening the multiple PI3K-AKT-mTOR targeted drugs under development for cancer treatment. Further investigation into alternative pathways downstream of AKT may reveal more specific targets. We continue to explore the cellular features common to all LM-LEC populations, as well as distinguishing differences, with the hope of identifying useful pathological profiles. Appreciating the unique genetics and underlying biochemical phenotype of LM-LECs would be instructive in the design of generally effective treatments, as well as personalized approaches as they are needed.

MATERIAL AND METHODS

Surgical specimens, cell isolation and culture

Tissue and fluid were obtained from patients undergoing surgical resection or sclerotherapy in the reductive treatment of LMs.

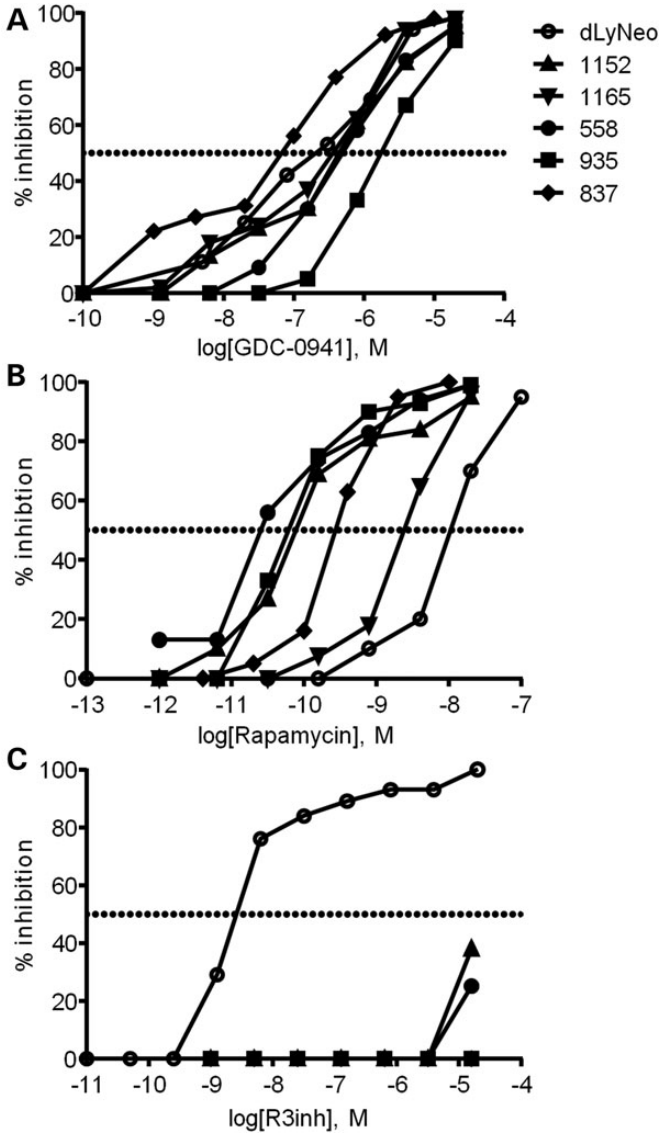

Figure 7 Susceptibility of LM-LECs to targeted inhibitors. Cultures of lesion-derived LECs were treated with drugs in EGM-2MV (**A** and **B**) or Red2MV (**C**) in triplicate wells, and proliferation determined by WST-1 assay after 2 or 4 days in culture. (A) PI3K inhibitor GDC-0941. (B) mTOR inhibitor rapamycin (sirolimus). (C) VEGFR3 inhibitor SAR131675. In (C), dLyNeo cultures were supplemented with 100 ng/ml VEGFC to demonstrate the efficacy of VEGFR3 inhibition; LM-LEC cultures were growth-factor-free and all patient cells but those of 1165 are plotted on the graph.

Table 2 All reported LMs were categorized with respect to general clinical descriptions

Clinical group	Samples (*n*) LEC/tissue	Mutation incidence (*n*)			
		E542K/A	E545K	H1047R/L	Unknown
LM, head and neck	5/2	2	3	2	0
LM, trunk or extremity	3/6	3	4	1	1
CVLM, no overgrowth	3/6	1	2	4	2
CVLM, with overgrowth	3/1	1	1	2	0

Numbers of samples bearing the indicated PIK3CA allele are presented. Direct sequencing was performed on LEC cultures whereas tissue samples were screened by ARMS-PCR. Twenty-six of 29 samples (89%) were identified as having an activating PIK3CA allele. E542 and H1047 allele pairs are combined as indicated. Unknown: a negative result after screening for the five common PIK3CA alleles. The three unknown samples corresponded to archived lesion samples.

Samples were obtained in accordance with the guidelines of the Institutional Review Board at CCHMC and with the written consent of the participants or guardians (protocol number 2011–2928). Surgical samples, delivered on ice from the operating room, were divided into portions that were flash frozen and stored at −80°C or processed immediately for the isolation of cells. Samples of fresh tissue were disrupted by collagenase treatment (0.1% collagenase type I; Worthington Biochemical Corp., NJ, USA) in DMEM for 2 h at 37°C under 5% CO_2, then passed through a nylon cell strainer (100 μm). Disaggregated cells, or cells suspended in lesion aspirates, were collected by centrifugation and expanded in EGM-2MV (Lonza Walkersville, Inc., Walkersville, MD, USA) by plating on fibronectin-coated plastic (20 μg/cm^2) and incubating at 37°C in humidified CO_2 (5%). Cultures were then collected by trypsinization and fractionated by immunomagnetic separation (MACS, Miltenyi Biotec Inc., Auburn, CA, USA) using CD31 antibody-coated magnetic beads (Miltenyi). CD31-positive cells were expanded further in EGM-2MV, and the CD31-negative fraction was expanded in DMEM supplemented with antibiotics and 10% FBS. LECs (designated passage 2) were derived from CD31+ endothelial cells by immunomagnetic selection for PDPN expression using rabbit anti-PDPN (Sigma-Aldrich, St. Louis, MO, USA) and goat anti-rabbit magnetic beads (Miltenyi). Lesion-derived LECs and neonatal dermal LECs (dLyNeo, Lonza) were routinely passaged in EGM-2MV. Primary cells were used experimentally at passages 4 through 7. Doubling times of plated cells in EGM-2MV or reduced medium (Red2MV: EGM-2MV less growth factors, 1% serum) were computed by direct cell counts using the formula T_d (doubling time) $= (\ln 2 \times T)/\ln(N_f/N_i)$, where T, total time; N_f = final cell number and N_i = initial cell number. Cells were plated at a density of 5×10^3/cm^2 and counted, in triplicate, on successive days.

Immunofluorescence and immunohistochemistry

For the identification and verification of LEC populations, cells were plated in multi-well chamber slides and immunostained following cold methanol fixation with rabbit anti-PDPN (p5374, Sigma-Aldrich) and rabbit anti-PROX1 (ab38692, Abcam, Cambridge, MA, USA) separately. Visualization was achieved using goat anti-rabbit Alexa Fluor 488 secondary antibody (Life Technologies, Grand Island, NY, USA). Nuclei were counterstained with DAPI fluorescent stain (Life Technologies). The immunostaining of tissue samples was performed on deparaffinized thin sections cut from formalin-fixed blocks embedded in paraffin. Serial sections were reacted with PROX1 antibody and αSMA antibody (Thermo Fisher Scientific, Waltham,

MA, USA) separately, and visualized with anti-rabbit HRP-conjugated secondary antibody followed by DAB peroxidase substrate (Vector Labs, Burlingame, CA, USA).

Angiogenic sprouting assay

The sprouting assay was based on a published procedure (42). Briefly, spheroids were formed from 1000 LECs suspended in Red2MV with 0.24% high viscosity methocel (Sigma-Aldrich) in the wells of a 96-well round-bottom plate. After 24 h of culture, the spheroids were collected by centrifugation, suspended in 1.5 mg/ml collagen type I (BD Biosciences, San Jose, CA, USA) containing 0.6% methocel, and cultured in Red2MV or Red2MV + VEGF-C (100 ng/ml). On average, 12 spheroids were embedded in 0.5 ml of collagen suspension per well of a prewarmed 24-well plate. Radial sprout lengths were digitally recorded using AxioVision version 4.8.2 software (Carl Zeiss Microscopy, Thornwood, NY, USA). Reported lengths are averages of three equally spaced diametric measurements of suspended spheroids (from sprout tip to sprout tip) less the diameter of the original spheroid.

Real-time PCR and protein expression analyses

LEC total RNA was isolated using the RNeasy Plus Mini kit (Qiagen Inc., Valencia, CA, USA) and reverse transcribed using the High Capacity cDNA kit (Life Technologies) from 2 μg of RNA. RT-qPCR was performed in 20 μl reactions with SYBR Premix Ex Taq II (Clontech Laboratories, Inc., Mountain View, CA, USA) in a CFX96 thermocycler (Bio-Rad Laboratories, Hercules, CA, USA) in triplicate reactions. The comparative threshold cycles (ΔΔCt) values were normalized to GAPDH using CFX manager software (version 3.0). Relative values were normalized to expression levels in dLyNeo cells. Primers, synthesized by Integrated DNA Technologies (Coralville, IA, USA), are listed in Supplementary Material, Table S1.

For protein expression, cells were lysed in RIPA buffer containing protease inhibitor cocktail (Santa Cruz Biotechnology, Dallas, TX, USA), sonicated briefly and clarified by centrifugation. Protein aliquots (5–20 μg) were fractionated by SDS–PAGE in 4–15% gels, blotted onto PVDF membranes (Bio-Rad) and probed with the following antibodies: rabbit anti-PTEN (#9188), rabbit anti-COX2 (#12282), rabbit anti-AKT (#4691), rabbit anti-phospho-AKT (#4060), rabbit anti-ERK1/2 (#4695) and rabbit anti-phospho-ERK1/2 (#4370) (Cell Signaling Technologies, Danvers, MA, USA), mouse anti-GAPDH (#10R-G109a, Fitzgerald Industries International, Acton, MA) and mouse anti-ANG2 (MAB0983, R&D Systems, Minneapolis, MN, USA). HRP-conjugated secondary antibodies and ECL substrate were obtained from Bio-Rad. Membranes were stripped with Restore Plus (Thermo Fisher) and probed repeatedly. VEGF-C in culture media was measured by ELISA (R&D Systems, Minneapolis, MN, USA).

DNA sequencing and cloning of PIK3CA sequences

PIK3CA mutations were confirmed by direct sequencing of PCR amplification products generated from targeted genomic sequences in isolated LM-LECs as previously reported (11). An alternative *PIK3CA* primer pair (Supplementary Material, Table S1) was used to amplify *PIK3CA* exon 9 to verify p.E545-related base substitutions. Relative abundance of wild-type and mutant E542K PIK3CA alleles in 1165 and 935 was estimated by isolation of genomic DNA from these cell populations and PCR amplification of exon 9 using Ex Taq (Clontech), 2 mM $MgCl_2$, 200 nM primers and 250 μM dNTPs. The 3′ A terminal overhang was removed using T4 polymerase (Thermo Fisher Scientific) in the presence of 250 μM dNTPs at 11°C for 20 min. The PCR product was then subcloned into the Zero Blunt TOPO PCR Cloning Kit for Sequencing (Life Technologies) and individual colonies were screened either by sequencing or by ARMS-PCR to determine whether the insert was wild-type, E542K mutant or pseudogene sequence from 22q11.2.

Screening for somatic mutations in archived tissue

LM samples were collected from the Cincinnati Children's Hospital Vascular Malformations Tissue Repository. Genomic DNA was isolated from 25 mg of frozen tissue using the PureLink DNA isolation kit (Life Technologies). Allele-specific PCR primers were designed for E542K, E545A, E545K, H1047L and H1047R mutations (see Supplementary Table 1) and used to test the isolated DNA by ARMS-PCR. E542K, E545K, H1047L and H1047R primers were designed based off previously published allele-specific primers (43) and their specificity confirmed by testing allele-containing gDNA identified by direct sequencing (Supplementary Material, Fig. S2).

Drug inhibition assays

Cell proliferation in the presence of inhibitors was measured by WST-1 assay (Clontech). Drugs (Rapamycin/Sirolimus, GDC-0941 and SAR131675; Selleck Chemicals, Houston, TX, USA) were dissolved in DMSO and serially diluted in growth medium. LECs were seeded at 1000–2000 cells per fibronectin-coated well of a 96-well plate in EGM-2MV and cultured in humidified 5% CO_2 at 37°C. For rapamycin and GDC-0941 measurements, drugs were added in EGM-2MV 2 h post-seeding. For SAR131675 inhibition studies, EGM-2MV was replaced after 16 h with Red2MV+/− VEGF-C (100 ng/ml) plus inhibitor. Cells were cultured for 48 or 96 h in the presence of drug, treated with WST-1 reagent and absorbance read after 30 and 60 min of culture at 37°C.

Statistical analyses

Inhibition plots were generated by GraphPad Prism version 6.01 (GraphPad Software). Significance was determined to $P < 0.05$ by one-way ANOVA analysis or Student's *t*-tests.

SUPPLEMENTARY MATERIAL

Supplementary Material is available at *HMG* online.

ACKNOWLEDGEMENTS

The authors thank Richard Azizkhan MD, chair of the Division of Pediatric Surgery and co-director of the Hemangioma and

Vascular Malformation Center, as well as Denise Adams MD, chair of Vascular Tumor Translational Research and co-director of the Hemangioma and Vascular Malformations Center at CCHMC, for internal financial support and fruitful discussions.

Conflict of Interest statement. The authors have no conflicts of interest, financial, intellectual, or otherwise, to declare.

FUNDING

This work was supported through internal funding provided by the Cincinnati Children's Hospital and Medical Center.

REFERENCES

1. Uebelhoer, M., Boon, L.M. and Vikkula, M. (2012) Vascular anomalies: from genetics toward models for therapeutic trials. *Cold Spring Harb. Perspect. Med.*, **2**, a006239.
2. Cahill, A.M. and Nijs, E.L. (2011) Pediatric vascular malformations: pathophysiology, diagnosis, and the role of interventional radiology. *Cardiovasc. Interv. Rad.*, **34**, 691–704.
3. Greene, A.K. (2012) Current concepts of vascular anomalies. *J. Craniofac. Surg.*, **23**, 220–224.
4. Shirley, M.D., Tang, H., Gallione, C.J., Baugher, J.D., Frelin, L.P., Cohen, M.D., North, P.E., Marchuk, D.A., Comi, A.N. and Pevsner, J.P. (2013) Sturge-Weber syndrome and port-wine stains caused by somatic mutation in *GNAQ*. *N.* Eng. J. Med., **368**, 1971–1979.
5. Vikkula, M., Boon, L.M., Carraway III, K.L., Calvert, J.T., Diamonti, A.J., Goumerov, B., Pasyk, K.A., Marchuk, D.A., Warman, M.L., Cantley, L.C. *et al.* (1996) Vascular dysmorphogenesis caused by an activating mutation in the receptor tyrosine kinase TIE2. *Cell*, **87**, 1181–1190.
6. Schulte-Merker, S., Sabine, A. and Petrova, T.V. (2011) Lymphatic vascular morphogenesis in development, physiology, and disease. *J. Cell Biol.*, **193**, 607–618.
7. Perkins, J.A., Manning, S.C., Tempero, R.M., Cunningham, M.J., Edmonds, J.L. Jr, Hoffer, F.A. and Egbert, M.A. (2010) Lymphatic malformations: current cellular and clinical investigations. *Otolaryng. Head Neck Surg.*, **142**, 789–794.
8. Blatt, J., McLean, T.W., Castellino, S.M. and Burkhart, C.N. (2013) A review of contemporary options for medical management of hemangiomas, other vascular tumors, and vascular malformations. *Pharmacol. Therapeut.*, **139**, 327–333.
9. Boardman, K.C. and Swartz, M.A. (2003) Interstitial flow as a guide for lymphangiogenesis. *Circ. Res.*, **92**, 801–808.
10. Planas-Paz, L., Strilic, B., Goedecke, A., Breier, G., Fassler, R. and Lammert, E. (2012) Mechanoinduction of lymph vessel expansion. *EMBO J.*, **31**, 788–804.
11. Kurek, K.C., Luks, V.L., Ayturk, U.M., Alomari, A.I., Fishman, S.J., Spencer, S.A., Mulliken, J.B., Bowen, M.E., Yamamoto, G.L., Kozakewich, H.P. *et al.* (2012) Somatic mosaic activating mutations in *PIK3CA* cause CLOVES syndrome. *Am. J. Hum. Genet.*, **90**, 1108–1115.
12. Baradaran-Heravi, A. (2012) *PIK3CA*, a hotspot for post-zygotic mutations in nonhereditary overgrowth syndromes. *Clin. Genet.*, **82**, 523–525.
13. Liu, N-F., Lu, Q. and Yan, Z-X. (2010) Lymphatic malformation is a common component of Klippel-Trenaunay syndrome. *J. Vasc. Surg.*, **52**, 1557–1563.
14. Cohen, C.M. (2013) Proteus syndrome review: molecular, clinical, and pathologic features. Clin. Genet., **85**, 111–119.
15. Lee, B.H., Kim, J.-M., Jin, H.Y., Kim, G-H., Choi, J.-H. and Yoo, H.-W. (2011) Spectrum of mutations in Noonan syndrome and their correlation with phenotypes. *J. Pediatr.*, **159**, 1029–1035.
16. Burrows, P.E., Gonzalez-Garay, M.L., Rasmussen, J.C., Aldrich, M.B., Guillod, R., Maus, E.A., Fife, C.E., Kwon, S., Lapinski, P.E., King, P.D. and Sevick-Muraca, E.M. (2013) Lymphatic abnormalities are associated with RASA1 gene mutations in mouse and man. Proc. Natl. Acad. Sci. USA, **110**, 8621–8626.
17. Alitalo, K. (2011) The lymphatic vasculature in disease. *Nat. Med.*, **17**, 1371–1380.
18. Makinen, T., Veikkola, T., Mustjoki, S., Karpanen, T., Catimel, B., Nice, E.C., Wise, L., Mercer, A., Kowalski, H., Kerjaschki, D. *et al.* (2001) Isolated lymphatic endothelial cells transduce growth, survival and migratory signals via the VEGF-C/D receptor VEGFR-3. *EMBO J.*, **20**, 4762–4773.
19. Wigle, J.T., Harvey, N., Detmar, M., Lagutina, I., Grosveld, G., Gunn, M.D., Jackson, D.G. and Oliver, G. (2002) An essential role for Prox1 in the induction of the lymphatic endothelial cell phenotype. *EMBO J.*, **21**, 1505–1513.
20. Kriehuber, E., Breiteneder-Geleff, S., Groeger, M., Soleiman, A., Schoppmann, S.F., Stingl, G., Kerjaschki, D. and Maurer, D. (2001) Isolation and characterization of dermal lymphatic and blood endothelial cells reveal stable and functionally specialized cell lineages. *J. Exp. Med.*, **194**, 797–808.
21. Kang, S., Bader, A.G. and Vogt, P.K. (2005) Phosphatidylinositol 3-kinase mutations identified in human cancer are oncogenic. Proc. Natl. Acad. Sci. *USA*, **102**, 802–807.
22. Stambolic, V., Suzuki, A., de la Pompa, J.L., Brothers, G.M., Mirtsos, C., Sasaki, T., Ruland, J., Penninger, J.M., Siderovski, D.P. and Mak, T.W. (1998) Negative regulation of PKB/Akt-dependent cell survival by the tumor suppressor PTEN. *Cell*, **95**, 29–39.
23. Mendoza, M.C., Er, E.E. and Blenis, J. (2011) The Ras-ERK and PI3K-mTOR pathways: cross-talk and compensation. *Trends Biochem. Sci.*, **36**, 320–328.
24. Coso, S., Zeng, Y., Opeskin, K. and Williams, E.D. (2012) Vascular endothelial growth factor receptor-3 directly interacts with phosphatidylinositol 3-kinase to regulate lymphangiogenesis. *PLoS ONE*, **7**, e39558.
25. Thurston, G. and Daly, C. (2012) The complex role of angiopoietin-2 in the angiopoietin-tie signaling pathway. *Cold Spring Harb. Perspect. Med.*, **2**, a006550.
26. Mouta-Bellum, C., Kirov, A., Miceli-Libby, L., Mancini, M.L., Petrova, T.V., Liaw, L., Prudovsky, I., Thorpe, P.E., Miura, N., Cantley, L.C. *et al.* (2009) Organ-specific lymphangiectasia, arrested lymphatic sprouting, and maturation defects resulting from gene-targeting of the PI3K regulatory isoforms p85alpha, p55alpha, and p50alpha. *Dev. Dynam.*, **238**, 2670–2679.
27. Karpanen, T. and Alitalo, K. (2008) Molecular biology and pathology of lymphangiogenesis. *Annu. Rev. Path.*, **3**, 367–397.
28. Zhuo, W., Jia, L., Song, N., Lu, X.A., Ding, Y., Wang, X., Song, X., Fu, Y. and Luo, Y. (2012) The CXCL12-CXCR4 chemokine pathway: a novel axis regulates lymphangiogenesis. *Clin. Cancer Res.*, **18**, 5387–5398.
29. Young, K., Conley, B., Romero, D., Tweedie, E., O'Neill, C., Pinz, I., Brogan, L., Lindner, V., Liaw, L. and Vary, C.P. (2012) BMP9 regulates endoglin-dependent chemokine responses in endothelial cells. *Blood*, **120**, 4263–4273.
30. Karnezis, T., Shayan, R., Fox, S., Achen, M.G. and Stacker, S.A. (2012) The connection between lymphangiogenic signalling and prostaglandin biology: a missing link in the metastatic pathway. *Oncotarget*, **3**, 890–903.
31. Folkes, A.J., Ahmadi, K., Alderton, W.K., Alix, X., Baker, S.J., Box, G., Chuckowree, I.S., Clarke, P.A., Depledge, P., Eccles, S.A. *et al.* (2008) The identification of 2-(1H-indazol-4-yl)-6-(4-methanesulfonyl-piperizan-1-ylmethyl)-4-morpholin-4-yl-thienol[3,2-d] pyrimidine (GDC-0941) as a potent, selective, orally available inhibitor of class I PI3 kinase for the treatment of cancer. *J. Med. Chem.*, **51**, 5522–5532.
32. Alam, A., Blanc, I., Gueguen-Dorbes, G., Duclos, O., Bonnin, J., Barron, P., Laplace, M.C., Morin, G., Gaujarengues, F., Dol, F. *et al.* (2012) SAR131675, a potent and selective VEGFR-3-TK inhibitor with antilymphangiogenic, antitumoral, and antimetastatic activities. *Mol. Cancer Therapeut.*, **11**, 1637–1649.
33. Bader, A.G., Kang, S., Zhao, L. and Vogt, P.K. (2005) Oncogenic PI3K deregulates transcription and translation. Nat. Rev. Cancer, **5**, 921–929.
34. Keppler-Noreuil, K.M., Sapp, J.C., Lindhurst, M.J., Parker, V.E.R., Blumhorst, C., Darling, T., Tosi, L.L., Huson, S.M., Whitehouse, R.W., Jakkula, E. *et al.* (2014) Clinical delineation and natural history of the *PIK3CA*-related overgrowth spectrum. *Am. J. Med. Genet. A*, **9999**, 1–21.
35. Boscolo, E., Mulliken, J.B. and Bischoff, J. (2013) Pericytes from infantile hemangioma display proangiogenic properties and dysregulated angiopoietin-1. *Arterioscler. Thromb. Vas. Biol.*, **33**, 501–509.
36. Choi, I., Lee, S. and Hong, Y.K. (2012) The new era of the lymphatic system: no longer secondary to the blood vascular system. *Cold Spring Harb. Perspect. Med.*, **2**, a006445.
37. Zhou, F., Chang, Z., Zhang, L., Hong, Y.K., Shen, B., Wang, B., Zhang, F., Lu, G., Tvorogov, D., Alitalo, K. *et al.* (2010) Akt/Protein kinase B is

required for lymphatic network formation, remodeling, and valve development. *Am. J. Pathol.*, **177**, 2124–2133.
38. Cheng, H.T. and Hung, W.C. (2013) Inhibition of proliferation, sprouting, tube formation and Tie2 signaling of lymphatic endothelial cells by the histone deacetylase inhibitor SAHA. *Oncol. Rep.*, **30**, 961–967.
39. Bachelor, M.A., Cooper, S.J., Sikorski, E.T. and Bowden, G.T. (2005) Inhibition of p38 mitogen-activated protein kinase and phosphatidylinositol 3-kinase decreases UVB-induced activator protein-1 and cyclooxygenase-2 in a SKH-1 hairless mouse model. *Mol. Cancer Res.*, **3**, 90–99.
40. Hutti, J.E., Pfefferle, A.D., Russell, S.C., Sircar, M., Perou, C.M. and Baldwin, A.S. (2012) Oncogenic PI3K mutations lead to NF-kappaB-dependent cytokine expression following growth factor deprivation. *Cancer Res.*, **72**, 3260–3269.
41. Courtois-Cox, S., Jones, S.L. and Cichowski, K. (2008) Many roads lead to oncogene-induced senescence. *Oncogene*, **27**, 2801–2809.
42. Korff, T. and Augustin, H.G. (1998) Integration of endothelial cells in multicellular spheroids prevents apoptosis and induces differentiation. *J. Cell Biol.*, **143**, 1341–1352.
43. Board, R.E., Thelwell, N.J., Ravetto, P.F., Little, S., Ranson, M., Dive, C., Hughes, A. and Whitcombe, D. (2008) Multiplexed assays for detection of mutations in PIK3CA. *Clin. Chem.*, **54**, 757–760.